



A Journal of the Gesellschaft Deutscher Chemiker

Angewandte Chemie

GDCh

International Edition

www.angewandte.org

Accepted Article

Title: Accelerating Electrochemical Reactions in a Voltage-Controlled Interfacial Microreactor

Authors: Heyong Cheng, Shuli Tang, Tingyuan Yang, Shiqing Xu, and Xin Yan

This manuscript has been accepted after peer review and appears as an Accepted Article online prior to editing, proofing, and formal publication of the final Version of Record (VoR). This work is currently citable by using the Digital Object Identifier (DOI) given below. The VoR will be published online in Early View as soon as possible and may be different to this Accepted Article as a result of editing. Readers should obtain the VoR from the journal website shown below when it is published to ensure accuracy of information. The authors are responsible for the content of this Accepted Article.

To be cited as: *Angew. Chem. Int. Ed.* 10.1002/anie.202007736

Link to VoR: <https://doi.org/10.1002/anie.202007736>

Accelerating Electrochemical Reactions in a Voltage-Controlled Interfacial Microreactor

Heyong Cheng,^[a, b] Shuli Tang,^[a] Tingyuan Yang,^[a] Shiqing Xu,^[a] and Xin Yan^{*[a]}

Abstract: Microdroplet chemistry is attracting increasing attention for accelerated reactions at the air/solution interface. We report here a novel voltage-controlled interfacial microreactor allowing acceleration of electrochemical reactions which are not observed in bulk or conventional electrochemical cells. The microreactor is formed at the interface of the Taylor cone in an electrospray emitter with a large orifice. This allows continuous contact of the electrode and the reactants at/near the interface. As a proof-of-concept, electro-oxidative C–H/N–H coupling and electro-oxidation of benzyl alcohol were shown to be accelerated by more than an order of magnitude compared to the corresponding bulk reactions. The new electrochemical microreactor has unique features that allow i) voltage-controlled acceleration of electrochemical reactions achieved by voltage-dependent formation of the interfacial microreactor; ii) “reversible” electrochemical derivatization; and iii) *in situ* mechanistic study and capture of key radical intermediates when coupled with mass spectrometry.

Microdroplets have recently emerged as a unique form of chemical reactor that has gained significant attention due to the interfacial chemistry that produces reaction acceleration.^[1] Many studies have shown that reactions in microdroplets exhibit acceleration of reaction rates by one or more orders of magnitude compared to the corresponding bulk reactions.^[2] This effect is associated with reactions at the solution–air interface, where partial solvation of the reagents is one factor that reduces the critical energy for reaction.^[1b] These findings have stimulated the applications of microdroplet chemistry in chemical derivatization,^[3] reaction mechanistic studies,^[4] high-throughput reaction screening,^[5] and rapid small-scale, green and sustainable synthesis.^[6]

Microdroplets are readily generated by various spray methods,^[1] drop-casting thin film,^[6d, 7] ultrasonic nebulization,^[6b] and Leidenfrost levitation.^[8] Electrospray ionization (ESI)-based microdroplets are most commonly used in performing accelerated reactions,^[1] where electrostatic force is applied to a solution of reaction mixture. The jet of finite conductivity, known as the Taylor cone, breaks up into a plume of charged droplets where increased surface areas of microdroplets allow the acceleration of reactions. It is worth noting that such spray-based microdroplet reactors can be directly coupled with a mass

spectrometer, therefore microdroplet reactions can be monitored in real time, and structures of intermediates and products as well as reaction kinetics can be analyzed *in situ*.^[1a, 1c]

Reactions that have been studied in microdroplets include C–C,^[6a, 9] C–N,^[2, 10] and C–O^[6c, 11] bond formation, however, up to now a large and significant category of reactions not demonstrated in microdroplets is the electrochemical reaction. Modern electrochemistry has undergone a revival during the last few decades that results in many benefits over traditional reagent-based transformations.^[12] For example, electricity is used instead of stoichiometric amounts of redox reagents for chemical conversions; oxidizing and reducing potentials can be precisely controlled to enable highly chemoselective transformations. In spite of these benefits, electrochemical reactions often suffer from long reaction times, typically around 2–38 h.^[13] Such an obstacle prevents them from wide and efficient use. Thus, we are motivated to develop a microreactor that can be used to accelerate electrochemical reactions.

The challenge of developing spray-based microdroplet reactors applicable to electrochemical reactions is obvious. In the ESI process, electrochemical reactions are terminated in microdroplets, because reactants in the electrosprayed microdroplets lose contact with the ESI electrode when droplets are formed.

ESI can be coupled with a separate electrochemical (EC) flow reactor^[14] or directly used as an electrochemical cell^[3c, 15] for various studies such as identification of reaction intermediates^[14d-f], examination of electrochemical reactions^[14a, 15b], and to mimic biologically relevant electrochemical reactions.^[16] However, the electrochemical reactions occurring in such electrochemical cells or ESI emitters reflect the reaction behavior in the bulk phase and do not possess the acceleration phenomenon. Molecules that are easy to oxidize or reduce by one-electron transfer can quickly form a predictable species in the ESI process and the scope of such reactions is very limited.^[15a] This approach does not apply to a broad range of slower reactions such as the transformations of Csp^3-H , Csp^2-H , $C=C$, $-OH$, and $C=O$ groups.

In this work, we develop a novel electrochemical interfacial microreactor that allows continuous contact of the electrode and reactants, and acceleration of electrochemical reactions in a confined volume (Figure 1). The unique microreactor is formed at the solution-air interface of the Taylor cone in the ESI emitter with a large (139 μm) orifice, when the spray voltage is tuned to form a meniscus that has a large surface area (4500 μm^2) using a low ESI flow rate (a few tens of nL min^{-1}). The reactants at or near the meniscus can receive or lose electrons from/to the electrode upon the application of voltage, and the reaction products are immediately formed at the interface. This feature is not found in the standard ESI source with a small orifice (less than 10 μm) nor conventional EC-MS. Moreover, the electrochemical interfacial reactor is voltage-dependent, and the occurrence of reactions can be controlled by tuning voltages.

[a] Dr. H. Cheng, S. Tang, T. Yang, Prof. S. Xu, Prof. X. Yan
Department of Chemistry,
Texas A&M University,
580 Ross St., College Station, TX 77845.
E-mail: xyan@tamu.edu

[b] Dr. H. Cheng
College of Material Chemistry and Chemical Engineering,
Hangzhou Normal University, Hangzhou, 311121, China

Supporting information for this article is given via a link at the end of the document. **(Please delete this text if not appropriate)**

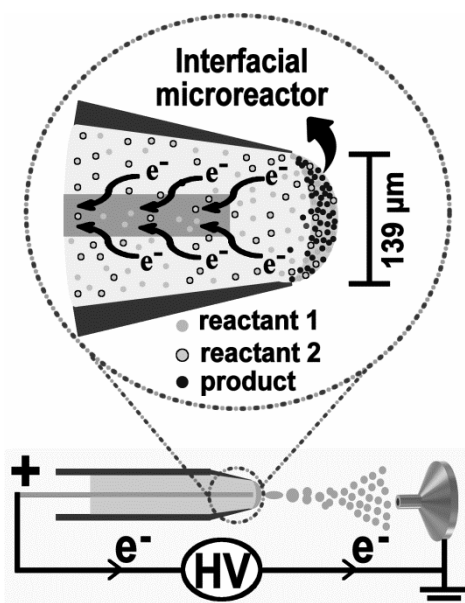
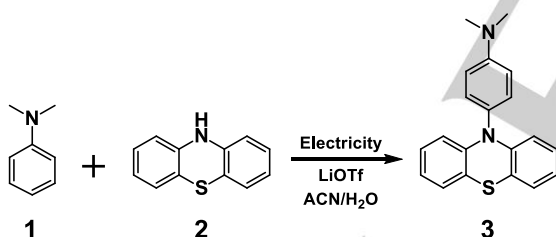


Figure 1. Schematic diagram of the interfacial microreactor for accelerating electrochemical reactions. The microreactor is formed at the solution-air interface of the Taylor cone in an ESI emitter with a large (139 μm) orifice, when the spray voltage (2 kV) is tuned to form a meniscus that has a large surface area (4500 μm^2) using a low ESI flow rate (a few tens of nL min^{-1}).

We demonstrate the feasibility of this electrochemical interfacial microreactor using the electro-oxidative C–H/N–H cross-coupling of *N,N*-dimethylaniline (DMA) and phenothiazine (PTA) (Scheme 1) as a proof-of-concept. Such a method of construction of aryl C–N bonds provides green and sustainable synthesis of various natural products, pharmaceuticals, agrochemicals and materials.^[17]



Scheme 1. Electro-oxidative C–H/N–H coupling of DMA (1) with PTA (2).

We dissolved DMA (1) (400 μM), PTA (2) (100 μM), and the electrolyte lithium triflate (LiOTf) (100 μM) in acetonitrile and water (1:1, v:v). The mixed solution was immediately loaded into the modified ESI emitter (orifice diameter of 139 μm) that was coupled with a mass spectrometer. Upon the application of a voltage of 2 kV to the ESI electrode (Pt), the large surface of meniscus was observed to be formed. A very fine spray of droplets was formed at the front of the meniscus and carried the reaction mixture to the MS inlet. The radical species of the coupling product (3) at m/z 318.1, and its in-source fragment ion at m/z 303.1 by the loss of methyl (Figure 2a) were observed immediately. The structures were confirmed by high resolution (Figure S2) and tandem mass spectra (Figure S3a) in comparison with the spectra of the purified product (Supporting Information S8). The signals of reactants PTA at m/z 199.1 and DMA dimer (*N,N,N',N'*-tetramethylbenzidine, TMB) at m/z 240

were less than 5% of the dominant product peak (m/z 318.1) after 7 s and remains constant. Two control experiments were performed. When no voltage was applied to the electrode, and the spray was initiated by pneumatic force (sonic spray), the reactants, PTA (m/z 199.1), its in-source fragment by the loss of sulfur (m/z 167.1), and DMA (m/z 122.1) were the major signals in the mass spectrum and no products were observed (Figure 2b). This result indicates that the C–H/N–H coupling was voltage-dependent. The corresponding bulk reaction was performed in an undivided electrochemical cell (see Supporting Information S1.4.2) using the same concentrations of the reactants and electrolytes, which led to the formation of product in a much lower intensity (Figure 2c and Figure S5). A large amount of PTA (m/z 199.1), its in-source fragment (m/z 167.1), and DMA (m/z 122.1) remained in the solution. The apparent acceleration factor (AAF, defined as the conversion ratio of products and reactants in microdroplet reaction versus that in bulk at the same reaction time)^[6d] was calculated to be 67. The above experiments demonstrate the acceleration of electro-oxidative C–H/N–H coupling in the newly developed electrochemical interfacial microreactor.

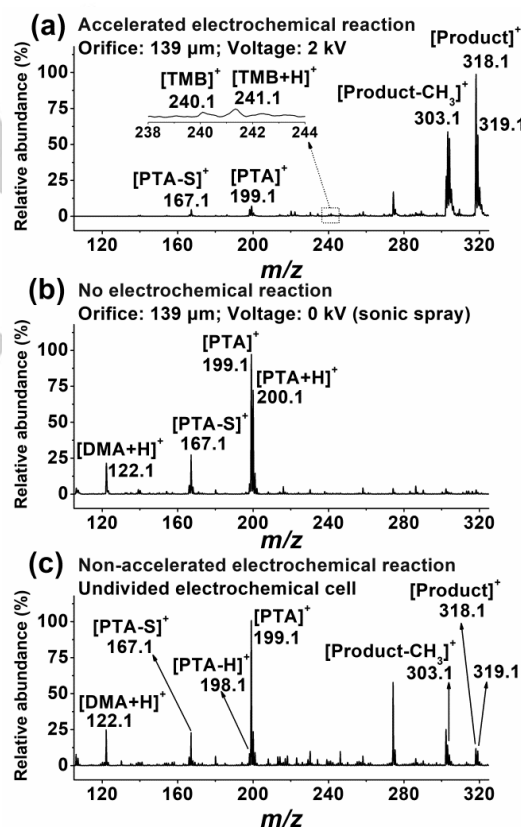


Figure 2. Mass spectra of the electro-oxidative coupling of PTA with DMA (a) in the interfacial microreactor at 7 s reaction time, (b) by sonic spray, and (c) in bulk at 7 s reaction time. The bulk reaction was performed in an undivided electrochemical cell (see Supporting Information S1.4.2 for the bulk reaction conditions and mass spectra collected at 5 min and 30 min reaction times). [Product-CH₃]⁺ and [PTA-S]⁺ are the in-source fragments. TMB is the DMA dimer.

The fact that the electrochemical interfacial microreactor is coupled with MS facilitates the study of reaction mechanisms by detecting transient intermediates. In previous work on the

mechanism of electro-oxidative C–H/N–H coupling of PTA and DMA,^[17] an electron paramagnetic resonance experiment was carried out to show reactant oxidation during electrolysis, while no further evidence was provided to demonstrate the reaction pathway.^[17] In our study, the key intermediates in accelerated electro-oxidative C–H/N–H coupling were captured by MS, and the mechanism is shown in Figure 3. DMA (**1**) was first oxidized to generate a radical cation (**4**). Homo-coupling of radical cation (**4**) could lead to the formation of its dimer TMB (**4a**). At the same time, **2** was also oxidized to generate a nitrogen radical (**5**) that can further lose one electron to form a nitrogen radical cation (**5a**). C–N bond was formed by radical/radical cross-coupling of radical cation (**4**) and nitrogen radical (**5**). Subsequent deprotonation of intermediate (**6**) afforded the final amination product (**3**). Our results provide direct evidence for the plausible mechanism proposed by the Lei group,^[17] demonstrating the power of the electrochemical microreactor with the capability of reaction mechanistic study.

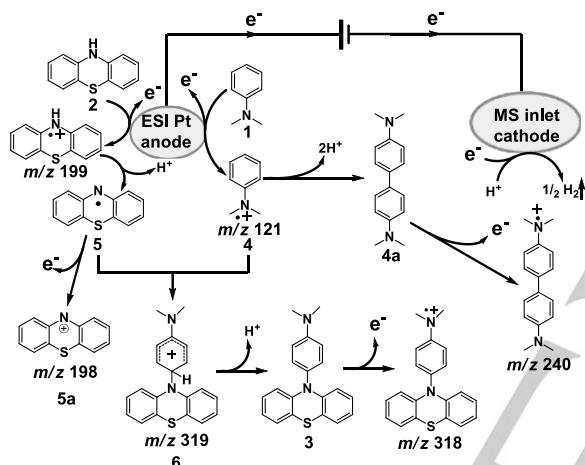


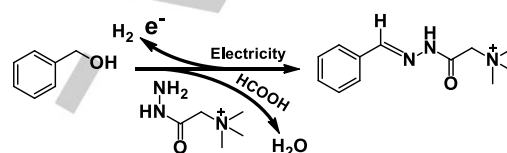
Figure 3. Plausible mechanism of electro-oxidative C–H/N–H coupling of DMA and PTA. The *m/z* of each intermediate and product observed in the mass spectra (Figure 2) is shown under its structure.

Encouraged by the accelerated electro-oxidative C–H/N–H coupling of DMA and PTA in the electrochemical microreactor, we quickly found other applications in online chemical transformations and demonstrated the unique feature of this microreactor in an on-demand chemical derivatization and *in situ* characterization of analytes that cannot be ionized and so cannot be studied by conventional mass spectrometry. The electrochemical reactions performed in the microreactor can be switched on/off by applying different ESI voltages. This was inspired by our recent work of locating double bonds in lipids using a voltage-dependent electro-epoxidation.^[3c]

Derivatization has been widely used in the analysis of chemicals that have no/low responses to mass analyzers due to their un-ionizable properties or low ionization efficiencies.^[18] Derivatization is commonly irreversible and one cannot switch between derivatized molecules and native molecules during a single analysis. The switchable feature of our microreactor makes the derivatization “reversible”, which allows one to observe the native and derivatized compounds in the same run. This might be beneficial to a mixture analysis in which some analytes need to be derivatized while others do not. The

switchable feature was realized by performing accelerated and non-accelerated electrochemical reactions during different voltages.

To prove this concept, we tested direct MS analysis of benzyl alcohol in the new electrochemical microreactor. Alcohols are not well detected using standard ESI-MS.^[12d, 19] Our strategy is to enable a one-step electro-oxidation of benzyl alcohol and couple it with Girard T (GT, a quaternary ammonium hydrazine salt) for *in-situ* formation of the charged hydrazone (BGT) (Scheme 2).^[20] Without performing the electrochemical reaction, benzyl alcohol was not detectable by MS with or without added GT reagent (Figure 4a). After we set the voltage to 2 kV, the derivatized benzyl alcohol in the form of the charged hydrazone (BGT) was detected immediately in the spectrum (Figure 4b). Compared with the bulk reaction (Figure S6), the electrochemical derivatization in the interfacial microreactor showed an apparent acceleration factor of 111. Then we tested the switchable feature by quickly changing the voltage between 2 kV (with interfacial reactor) and



Scheme 2. Electrochemical derivatization of benzyl alcohol with GT reagent in the electrochemical interfacial microreactor.

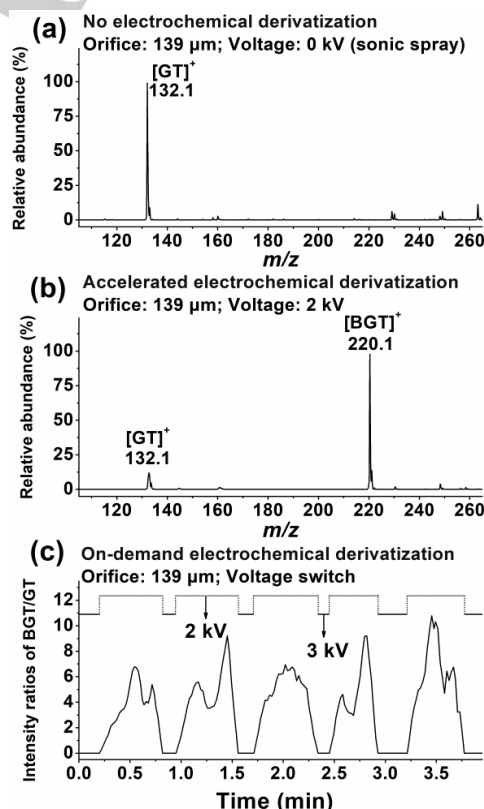


Figure 4. Mass spectra showing a one-step electrochemical derivatization of benzyl alcohol in the presence of GT reagent (a) by sonic spray without applying voltage; and (b) in the interfacial microreactor. (c) Chronogram of the MS intensity ratio of BGT to GT upon varying the ESI voltage between 2 kV and 3 kV, showing the rapid switchable electrochemical derivatization in the microreactor.

3 kV (normal ESI without interfacial reactor) (Figure 4c). The chronogram of MS intensity ratio of derivatized benzyl alcohol (BGT) to GT reagent vs. time shows that the electrochemical derivatization of benzyl alcohol was turned on at 2 kV and turned off at 3 kV. This result further confirms that electrochemical reactions can be significantly accelerated in the interfacial microreactor, and provides an example of switchable electrochemical derivatization for chemical analysis as well.

To clarify the inherent mechanism for acceleration in the electrochemical interfacial microreactor, attention was paid to the geometry of the meniscus formed in the ESI process that is specific to the spraying mode, and is dependent on the voltage, flow rate, and orifice diameter. As shown by the microscopic images (Figure S14) and the videos (Table S2) recorded by a microscopic camera, the electro spray from an emitter of a 139 μm orifice successively underwent the dripping, microdripping, spindle, cone jet (standard ESI mode) and multijet modes when the applied voltage was increased from 1.85 kV to 3.50 kV. We observed that the electrochemical reactions could be accelerated most in the microdripping mode (Supporting Information S6) which maintains a large surface area (Figure 5a and b). In the ESI with an orifice less than 10 μm , however, the electro spray immediately responded to the cone jet without the other modes (dripping, microdripping and spindle) on gradually increasing the voltage (Figure 5c and d), which led to no obvious accelerated reactions in those ESI emitters. This indicates that the interfacial effect of the large-area meniscus in the microdripping mode of electro spray plays a key role in the accelerated electrochemical reactions. Similar results have been observed in additional reactions (Supporting Information S3-S5).

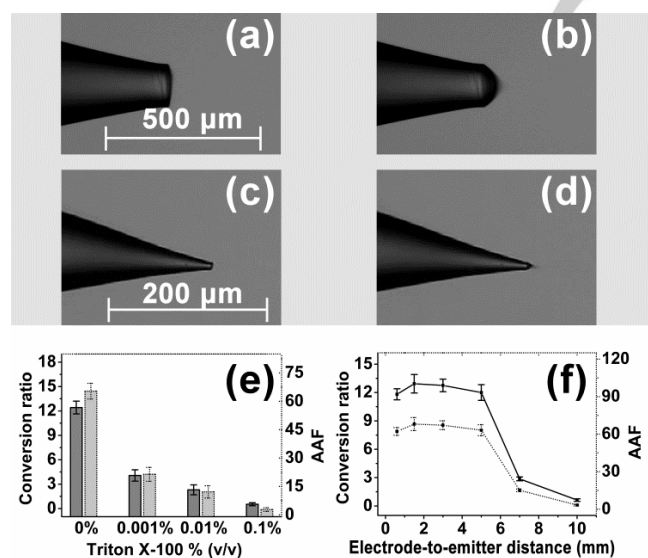


Figure 5. Microscopic images showing the ESI tip shapes of a 139 μm -emitter (a) before spraying, (b) in the microdripping mode; the ESI tip shapes of a 3 μm -emitter (c) before spraying and (d) in the cone-jet mode; (e) Effects of Triton X-100 (% represents volume of Triton X-100/volume of reaction solution) on the conversion ratios (solid black) and apparent acceleration factors (AAFs, dotted gray) of the electrochemical coupling of PTA with DMA in the interfacial microreactor; (f) Effects of the electrode-to-interface distance on the conversion ratios (solid) and AAFs (dotted) of the electrochemical coupling of PTA with DMA in the interfacial microreactor. The measurement of each accelerated reaction was repeated 5 times. The error bars represent the standard deviation of five measurements.

Furthermore, we added a neutral surfactant Triton X-100 to the electrochemical reaction of PTA and DMA in the interfacial microreactor. With the increased amount of Triton X-100 (from 0.001% to 0.1%, v/v), we observed decreased conversion ratios and acceleration factors (Figure 5e), which further demonstrates the role of the interface in reaction acceleration as Triton X-100 blocks the surface and diminishes accelerated product formation (see Supporting Information S7.4). Then we changed the distance between the ESI emitter and the MS inlet to vary the possible reaction time in the electro sprayed microdroplets. The reaction conversions of the electrochemical coupling of PTA and DMA were similar at different distances (Figure S16), which suggests that the electrochemical reaction acceleration does not occur to a major extent in the electro sprayed microdroplets, but at the interface of the Taylor cone. In addition, we found that the distance between the electrode and air/solution interface of the Taylor cone is very important in the electrochemical interfacial reactor. A distance of 0.6–5 mm allows the reactants at or near the interface to receive or lose electrons from/to the electrode upon the application of voltage (Figure 5f, SI section 7.2). The above results suggest that the electrochemical reaction is initiated at the electrode and is accelerated at the air/solution interface close to the electrode.

In conclusion, we present a novel voltage-controlled interfacial microreactor that can accelerate electrochemical reactions. This microreactor is formed at the solution-air interface of the Taylor cone in the ESI emitter of a 139 μm orifice. The electro-oxidative C–H/N–H coupling of DMA and PTA, and electrochemical derivatization of benzyl alcohol performed in such an electrochemical microreactor show the acceleration factors of 67 and 111 compared to the corresponding bulk reactions, respectively. The coupling of microreactors with MS allows us to capture the key radical intermediates in a mechanistic study of electro-oxidative C–H/N–H coupling of DMA and PTA. The electrochemical derivatization can be switched on and off by changing the spray voltage, which allows the collection of mass spectra before and after derivatization in a single run. The demonstrated fast electrochemical transformations, on-demand derivatization and *in situ* mechanistic study allow this novel interfacial microreactor a wide use in the electrochemistry related research.

Acknowledgements

We acknowledge the support and start-up funds from Texas A&M University and the Department of Chemistry. Dr. Heyong Cheng appreciates the financial support from the National Natural Science Foundation of China under project No. 21974048. We thank for the help from Dr. Zhenwei Wei with the TOC figure.

Conflict of interest

The authors declare no conflict of interest.

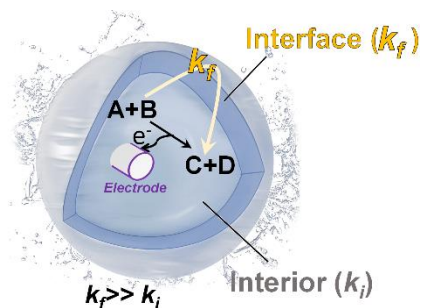
Keywords: interfacial microreactor • electrochemical reaction • electrospray • reaction acceleration • mass spectrometry

References

- [1] a) R. G. Cooks, X. Yan, *Ann. Rev. Anal. Chem.* **2018**, *11*, 1-28; b) Z. Wei, Y. Li, R. G. Cooks, X. Yan, *Ann. Rev. Phys. Chem.* **2020**, *71*, 31-51; c) X. Yan, R. M. Bain, R. G. Cooks, *Angew. Chem. Int. Ed.* **2016**, *55*, 12960-12972.
- [2] a) R. M. Bain, C. J. Pulliam, R. G. Cooks, *Chem. Sci.* **2015**, *6*, 397-401; b) S. Banerjee, R. N. Zare, *Angew. Chem. Int. Ed.* **2015**, *54*, 14795-14799.
- [3] a) W. Cao, S. Cheng, J. Yang, J. Feng, W. Zhang, Z. Li, Q. Chen, Y. Xia, Z. Ouyang, X. Ma, *Nat. Commun.* **2020**, *11*, 375; b) W. Zhang, D. Zhang, Q. Chen, J. Wu, Z. Ouyang, Y. Xia, *Nat. Commun.* **2019**, *10*, 79; c) S. Tang, H. Cheng, X. Yan, *Angew. Chem. Int. Ed.* **2020**, *59*, 209-214; d) Z. Wei, X. Zhang, J. Wang, S. Zhang, X. Zhang, R. G. Cooks, *Chem. Sci.* **2018**, *9*, 7779-7786; e) X. Ma, L. Chong, R. Tian, R. Shi, T. Y. Hu, Z. Ouyang, Y. Xia, *Proc. Natl. Acad. Sci. U.S.A.* **2016**, *113*, 2573; f) X. Ma, Y. Xia, *Angew. Chem. Int. Ed.* **2014**, *53*, 2592-2596.
- [4] a) S. Banerjee, S. Sathyamoorthi, J. Du Bois, R. N. Zare, *Chem. Sci.* **2017**, *8*, 7003-7008; b) S. Chen, Q. Wan, A. K. Badu-Tawiah, *Angew. Chem. Int. Ed.* **2016**, *55*, 9345-9349; c) S. Banerjee, C. Basheer, R. N. Zare, *Angew. Chem. Int. Ed.* **2016**, *55*, 12807-12811; d) X. Yan, E. Sokol, X. Li, G. Li, S. Xu, R. G. Cooks, *Angew. Chem. Int. Ed.* **2014**, *53*, 5931-5935.
- [5] a) M. Wlekinski, B. P. Loren, C. R. Ferreira, Z. Jaman, L. Avramova, T. J. P. Sobreira, D. H. Thompson, R. G. Cooks, *Chem. Sci.* **2018**, *9*, 1647-1653; b) B. P. Loren, M. Wlekinski, A. Koswara, K. Yammine, Y. Hu, Z. K. Nagy, D. H. Thompson, R. G. Cooks, *Chem. Sci.* **2017**, *8*, 4363-4370.
- [6] a) H. G. Nie, Z. W. Wei, L. Q. Qiu, X. S. Chen, D. T. Holden, R. G. Cooks, *Chem. Sci.* **2020**, *11*, 2356-2361; b) C. Liu, J. Li, H. Chen, Richard N. Zare, *Chem. Sci.* **2019**, *10*, 9367-9373; c) X. Yan, Y.-H. Lai, R. N. Zare, *Chem. Sci.* **2018**, *9*, 5207-5211; d) Z. Wei, M. Wlekinski, C. Ferreira, R. G. Cooks, *Angew. Chem. Int. Ed.* **2017**, *56*, 9386-9390.
- [7] a) A. K. Badu-Tawiah, D. I. Campbell, R. G. Cooks, *J. Am. Soc. Mass Spectrom.* **2012**, *23*, 1461-1468; b) Y. Li, X. Yan, R. G. Cooks, *Angew. Chem. Int. Ed.* **2016**, *55*, 3433-3437.
- [8] R. M. Bain, C. J. Pulliam, F. Thery, R. G. Cooks, *Angew. Chem. Int. Ed.* **2016**, *55*, 10478-10482.
- [9] a) K. Luo, J. Li, Y. Cao, C. Liu, J. Ge, H. Chen, R. N. Zare, *Chem. Sci.* **2020**, *11*, 2558-2565; b) T. Müller, A. Badu-Tawiah, R. G. Cooks, *Angew. Chem. Int. Ed.* **2012**, *51*, 11832-11835.
- [10] a) E. Gnanamani, X. Yan, R. N. Zare, *Angew. Chem. Int. Ed.* **2020**, *59*, 3069-3072; b) N. Sahota, D. I. AbuSalim, Melinda L. Wang, C. J. Brown, Z. Zhang, T. J. El-Baba, S. P. Cook, D. E. Clemmer, *Chem. Sci.* **2019**, *10*, 4822-4827; c) R. M. Bain, S. Sathyamoorthi, R. N. Zare, *Angew. Chem. Int. Ed.* **2017**, *56*, 15083-15087.
- [11] a) X. Yan, H. Cheng, R. N. Zare, *Angew. Chem. Int. Ed.* **2017**, *56*, 3562-3565; b) J. K. Lee, D. Samanta, H. G. Nam, R. N. Zare, *J. Am. Chem. Soc.* **2019**, *141*, 10585-10589; c) D. Gao, F. Jin, J. K. Lee, R. N. Zare, *Chem. Sci.* **2019**, *10*, 10974-10978; d) J. K. Lee, K. L. Walker, H. S. Han, J. Kang, F. B. Prinz, R. M. Waymouth, H. G. Nam, R. N. Zare, *Proc. Natl. Acad. Sci. U.S.A.* **2019**, *116*, 19294-19298.
- [12] a) Y. Jiang, K. Xu, C. Zeng, *Chem. Rev.* **2018**, *118*, 4485-4540; b) M. D. Kärkäs, *Chem. Soc. Rev.* **2018**, *47*, 5786-5865; c) M. Yan, Y. Kawamata, P. S. Baran, *Chem. Rev.* **2017**, *117*, 13230-13319; d) C. Wu, D. R. Iffa, N. E. Manicke, R. G. Cooks, *Anal. Chem.* **2009**, *81*, 7618-7624; e) X. Zhao, H. Ren, L. Luo, *Langmuir* **2019**, *35*, 5392-5408.
- [13] a) J. Luo, B. Hu, W. Wu, M. Hu, T. Liu, *Ni-Catalyzed Electrochemical C(sp²)-C(sp³) Cross-Coupling Reactions*, **2020**; b) J. Wu, Y. Dou, R. Guillot, C. Kouklovsky, G. Vincent, *J. Am. Chem. Soc.* **2019**, *141*, 2832-2837; c) Q.-L. Yang, Y.-Q. Li, C. Ma, P. Fang, X.-J. Zhang, T.-S. Mei, *J. Am. Chem. Soc.* **2017**, *139*, 3293-3298; d) Q.-L. Yang, X.-Y. Wang, J.-Y. Lu, L.-P. Zhang, P. Fang, T.-S. Mei, *J. Am. Chem. Soc.* **2018**, *140*, 11487-11494.
- [14] a) P. Khanipour, M. Löffler, A. M. Reichert, F. T. Haase, K. J. J. Mayrhofer, I. Katsounaros, *Angew. Chem. Int. Ed.* **2019**, *58*, 7273-7277; b) H. Cheng, X. Yan, R. N. Zare, *Anal. Chem.* **2017**, *89*, 3191-3198; c) Z. Wang, Y. Zhang, B. Liu, K. Wu, S. Thevuthasan, D. R. Baer, Z. Zhu, X.-Y. Yu, F. Wang, *Anal. Chem.* **2017**, *89*, 960-965; d) T. A. Brown, H. Chen, R. N. Zare, *Angew. Chem. Int. Ed.* **2015**, *54*, 11183-11185; e) T. A. Brown, H. Chen, R. N. Zare, *J. Am. Chem. Soc.* **2015**, *137*, 7274-7277; f) T. A. Brown, N. Hosseini-Nassab, H. Chen, R. N. Zare, *Chem. Sci.* **2016**, *7*, 329-332.
- [15] a) Q. Wan, S. Chen, A. K. Badu-Tawiah, *Chem. Sci.* **2018**, *9*, 5724-5729; b) K. Yu, H. Zhang, J. He, R. N. Zare, Y. Wang, L. Li, N. Li, D. Zhang, J. Jiang, *Anal. Chem.* **2018**, *90*, 7154-7157.
- [16] a) T. Herl, F.-M. Matysik, *Anal. Chem.* **2020**, *92*, 6374-6381; b) T. Zhang, M. P. de Vries, H. P. Permentier, R. Bischoff, *Anal. Chem.* **2017**, *89*, 7123-7129; c) I. Iftikhar, K. M. A. El-Nour, A. Brajter-Toth, *Electrochimica Acta* **2017**, *249*, 145-154; d) F. T. G. van den Brink, T. Zhang, L. Ma, J. Bomer, M. Odijk, W. Olthuis, H. P. Permentier, R. Bischoff, A. van den Berg, *Anal. Chem.* **2016**, *88*, 9190-9198.
- [17] K. Liu, S. Tang, T. Wu, S. Wang, M. Zou, H. Cong, A. Lei, *Nat. Commun.* **2019**, *10*, 639.
- [18] T. Huang, M. R. Armbruster, J. B. Coulton, J. L. Edwards, *Anal. Chem.* **2019**, *91*, 109-125.
- [19] S. T. Ayrtton, R. G. Cooks, M. Pugia, *Analyst* **2016**, *141*, 5398-5403.
- [20] a) M. Girod, E. Moyano, D. I. Campbell, R. G. Cooks, *Chem. Sci.* **2011**, *2*, 501-510; b) D. Wang, P. Wang, S. Wang, Y.-H. Chen, H. Zhang, A. Lei, *Nat. Commun.* **2019**, *10*, 2796.
- [21] X. Yan, R. Augusti, X. Li, R. G. Cooks, *ChemPlusChem* **2013**, *78*, 1142-1148.

Table of Contents

COMMUNICATION



Heyong Cheng, Shuli Tang, Tingyuan Yang, Shiqing Xu, and Xin Yan

Page No. – Page No.

Accelerating Electrochemical Reactions in a Voltage-Controlled Interfacial Microreactor

A novel interfacial microreactor was developed to achieve accelerated electrochemical reactions. The formation of the interfacial microreactor can be voltage-dependent and used for on-demand electrochemical derivatization and *in-situ* mechanistic study of electrochemical reactions.